New Chiral Palladium(0) and -(II) Complexes of (Aminoferrocenyl)phosphine Ligands PPFA and PTFA. X-ray Crystal Structure Analysis and Fluxional Behavior Involving Alkene Rotation, Pd−N Bond Rupture, and Selective $\eta^3-\eta^1-\eta^3$ Allyl Isomerization

Rafael Fernández-Galán, Félix A. Jalón, Blanca R. Manzano,*,† and Jerónimo Rodríguez-de la Fuente

Departamento de Química Inorgánica, Orgánica y Bioquímica, Facultad de Químicas, Campus Universitario, 13071 Ciudad Real, Spain

Miranda Vrahami, Brigitte Jedlicka, and Walter Weissensteiner*,‡

Institut für Organische Chemie, Universität Wien, Währingerstrasse 38, A-1090 Wien, Austria

Gerwald Jogl§

Institut für Physikalische Chemie, Universität Graz, Heinrichstrasse 28, A-8010 Graz, Austria

Received December 9, 1996⊗

(Aminoferrocenyl)phosphine ligands 2-(1-(dimethylamino)ethyl)-1-(diphenylphosphino)-ferrocene (PPFA) and [η^5-cyclopentadienyl][η^5-4-(*endo*-dimethylamino)-3-(diphenylphosphino)-4,5,6,7-tetrahydro-1*H*-indenyl]iron(II) (PTFA), were used as ligands in palladium(0) and -(II) complexes. The reaction of $Pd_2(dba)_3{\cdot}CHCl_3$ with PPFA or PTFA in the presence of the electron-withdrawing olefins maleic anhydride (MA) and dimethyl fumarate (DMFU) gave the complexes Pd(PTFA)(DMFU) (**2**), Pd(PPFA)(MA) (**3**), and Pd(PPFA)(DMFU) (**4**). Allylic complexes [Pd(η^3-2-Me-C_3H_4)(PTFA)]Tf (**5**) and [Pd(η^3-2-Me-C_3H_4)(PPFA)]Tf (**6**) (Tf = triflate) were obtained by reaction of PTFA or PPFA with [Pd(η^3-2-Me-C_3H_4)Cl]$_2$ in the presence of AgTf. In solution all these compounds exist as mixtures of two diastereomers, with either the alkene or the allyl group differently oriented with respect to the aminophosphine ligand. ^{1}H NMR variable-temperature studies have been carried out for **2**−**6** and for Pd(PTFA)-(MA) (**1**). Rotation of the alkene was observed for complexes **1**−**4** on the NMR time scale. $\Delta G^{\ddagger}_c$ has been calculated and values between 57.6 kJ mol^{-1} (298 K) and 76.6 kJ mol^{-1} (373 K) have been obtained. A Pd−N bond rupture which interchanges the two amino methyl groups is observed ($\Delta G^{\ddagger}_{328}$ = 63.9 kJ mol^{-1} to $\Delta G^{\ddagger}_{368}$ = 74.9 kJ mol^{-1}) for derivatives of PPFA, but not for complexes containing PTFA. An EXSY experiment carried out on complex **5** has evidenced a selective $\eta^3-\eta^1-\eta^3$ (carbon *cis* to phosphorus) allyl isomerization. Molecular structures of **4** and **6** were determined by X-ray structure analysis.

Introduction

During the last few years bi- and multifunctional ferrocene derivatives have been used successfully as ligands of homogeneous catalysts,[1] and further development of new ligands is still in progress. Ferrocenyl-based ligands have been tested in a number of enantioselective reactions such as hydrogenation, hydrosilylation, cross-coupling reactions, addition of dialkylzinc to aldehydes, aldol type condensations, and others.[2−4] Almost all of these derivatives are based on enantiopure (1-(dimethylamino)ethyl)ferrocene, which originally was developed by Ugi's group.[5] Ortho lithiation and subsequent reaction with electrophiles leads to a variety of bis- or tris-substituted ferrocenes such as the widely used 2-(1-(dimethylamino)ethyl)-1-(diphenylphosphino)-ferrocene (PPFA; Chart 1). The additional possibility of exchanging the dimethylamino group by other nucleophiles allows for a very high synthetic flexibility.[6,7]

Recently, we have studied new amino alcohols[8,9] and amino phosphines[10] such as PTFA (Chart 1), all derived from hetero- or homoannularly bridged ferrocenyl amines. In these ligands, the conformational flexibility, espe-

† E-mail: bmanzano@qino-cr.uclm.es.
‡ E-mail: Walter.Weissensteiner@univie.ac.at.
§ E-mail: jogl@bpch18.kfunigraz.ac.at.
⊗ Abstract published in *Advance ACS Abstracts,* July 15, 1997.

(1) Togni, A., Hayashi, T., Eds. *Ferrocenes*; VCH: Weinheim, Germany, 1995.
(2) Brunner, H.; Zettlmeier, W. *Handbook of Enantioselective Catalysis with Transition Metal Compounds*; VCH: Weinheim, Germany, 1993.
(3) Sawamura, M.; Ito, Y. *Chem. Rev.* **1992**, *92*, 857.
(4) Ojima, I., Ed., *Catalytic Asymmetric Synthesis*; VCH: Weinheim, Germany, 1993.
(5) Marquarding, D.; Klusacek, H.; Gokel, G.; Hoffmann, P.; Ugi, I. *J. Am. Chem. Soc.* **1970**, *92*, 5389.
(6) Hayashi, T.; Yamamoto, K.; Kumada, M. *Tetrahedron Lett.* **1974**, 4405.
(7) Hayashi, T.; Mise, T.; Fukushima, M.; Kagotani, M.; Nagashima, N.; Hamada, Y.; Matsumoto, A.; Kawakami, S.; Konishi, M.; Yamamoto, K.; Kumada, M. *Bull. Chem.. Soc. Jpn.* **1980**, *53*, 1138.
(8) Wally, H.; Kratky, C.; Weissensteiner, W.; Widhalm, M.; Schlögl, K. *J. Organomet. Chem.* **1993**, *450*, 185.
(9) Wally, H.; Schlögl, K.; Weissensteiner, W.; Widhalm, M. *Tetrahedron: Asymmetry* **1993**, *4*, 285.
(10) Jedlicka, B.; Kratky, C.; Weissensteiner, W.; Widhalm, M. *J. Chem. Soc., Chem. Commun.* **1993**, 1329.

S0276-7333(96)01035-7 CCC: $14.00

Chart 1. Configuration for the PPFA and PTFA Ligands

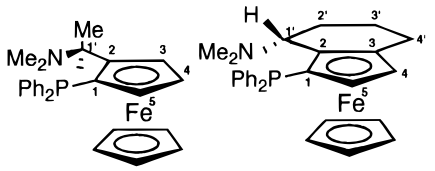

(S_c,R_m)-PPFA (R_c,R_m)-PTFA

cially of the dimethylamino group, is significantly reduced as compared to derivatives of PPFA, a fact which in an enantioselective catalytic reaction could favor higher enantioselectivities.

In the Grignard cross-coupling of vinyl bromide with phenethylmagnesium chloride, an enantioselectivity of 79% ee was achieved with use of PTFA−$PdCl_2$[10] as compared to 68% for PPFA−$PdCl_2$.

Only in a small number of papers have investigations on the reaction mechanism and especially on the enantioselective step of this cross-coupling reaction been reported.[11−13] However, it is assumed that the enantioselectivity is established during the transmetalation step, in which the phenylethyl group is transferred from the Grignard reagent onto the palladium catalyst. According to a proposal by Kumada and Hayashi,[14] this step is expected to involve bond cleavage of the palladium−nitrogen bond and coordination of the Grignard reagent to the amino substituent prior to the transfer of the alkyl group from magnesium to palladium. Although in the case of palladium complexes of (aminoferrocenyl)phosphines there is not any direct experimental evidence available for such a particular process, recently, for different types of ligands, fluxional processes involving Pd−N bond rupture have been described.[15] Furthermore, in a recent paper on pyrazole−ferrocenyl complexes Togni et al.[16] described an electronic effect on the enantioselectivity in rhodium-catalyzed hydroboration processes. It was found that higher enantioselectivities are obtained when both the N-ligand is a good σ-donor and the P-ligand a good π-acceptor. It was suggested that in the catalysis process a partial dissociation of the ligand from rhodium might be responsible for the lower enantioselectivity observed when catalysts with electron-withdrawing pyrazolyl ligands were used. Hence, it was of interest to search for direct evidence of such a decoordination process and to especially investigate the possibility of a Pd−N bond rupture in PPFA and PTFA palladium complexes, all potential Grignard cross-coupling catalysts or catalyst precursors.

In this paper we describe the synthesis, some structural aspects, and a study of the fluxional behavior of palladium(0) complexes of PPFA and PTFA with maleic anhydride (MA) and dimethyl fumarate (DMFU), as well as a study of the related (2-methylallyl)palladium(II) complexes. All compounds serve as models for the actual intermediates in a particular catalytic reaction. The olefins of the palladium(0) species have been chosen for the following reasons: (i) their electron-withdrawing ability is expected to lead to a sufficient stabilization in order to allow for a variable-temperature NMR study at elevated temperatures; (ii) distinct electron-accepting properties and consequently back-donation will alter the electronic properties of the palladium center as well as possible fluxional processes differently; (iii) usually, the alkene resonances are easily discernible in the NMR spectra; (iv) their different structural properties are expected to impose different local steric interactions onto the coordination site, thus providing complementary information about feasible fluxional processes.

Results and Discussion

Synthesis. According to eq 1, reaction of $Pd_2(dba)_3 \cdot CHCl_3$ in toluene with the (aminoferrocenyl)phosphine species (N-P) PPFA or PTFA (Chart 1) and with electron-poor olefins (L) maleic anhydride (MA) or dimethyl fumarate (DMFU) gave the new palladium(0) complexes of formula Pd(N-P)L (complex **1** has already been described by us in a previous paper[17]).

$$Pd_2(dba)_3 \cdot CHCl_3 + 2\text{N-P} + 2\text{L} \rightarrow 2\text{Pd(N-P)L} + 3\text{dba} \quad (1)$$

1−**4**

N-P	L	complex
PTFA	MA	1
PTFA	DMFU	2
PPFA	MA	3
PPFA	DMFU	4

The corresponding allyl complexes were obtained from the reaction of $[Pd(\eta^3\text{-2-Me-}C_3H_4)Cl]_2$ with the appropriate amino phosphine ligand in the presence of silver triflate according to the method described in the literature for other ligands[18a−c] (eq 2).

$$[Pd(\eta^3\text{-}C_4H_7)Cl]_2 + 2\text{N-P} + 2\text{AgTf} \rightarrow 2\,[Pd(\eta^3\text{-}C_4H_7)(\text{N-P})]\text{Tf} + 2\text{AgCl} \quad (2)$$

5,**6**

5, N-P = PTFA; **6**, N-P = PPFA

NMR Characterization of the New Palladium Complexes. We have found that **1**−**6** exist in solution always as a mixture of two diastereomers (see Chart 2), which differ in the way how either the alkene or the allyl group is oriented with respect to the amino phosphine ligand. When the solutions are prepared at low temperature from crystalline samples, for each of the DMFU complexes (**2** and **4**) only an unique isomer is seen. At room temperature, in each case, a second diastereomer evolves until an isomer equilibrium is reached. For related amino phosphine palladium de-

(11) Baker, K. V.; Brown, J. M.; Cooley, N. A.; Hughes, G. D.; Taylor, R. J. *J. Organomet. Chem.* **1993**, *370*, 397.
(12) Brown, J. M.; Cooley, N. A. *Chem. Rev.* **1988**, *88*, 1031.
(13) Indolese, A.; Consiglio, G. *J. Organomet. Chem.* **1993**, *463*, 23.
(14) Hayashi, T.; Kumada, M. *Acc. Chem. Res.* **1982**, *15*, 395.
(15) (a) Gogoll, A.; Örnebro, J.; Grennberg, H.; Bäckvall, J. E. *J. Am. Chem. Soc.* **1994**, *116*, 3631. (b) Albinati, A.; Kunz, R. W.; Amman, C. J.; Pregosin, P. S. *Organometallics* **1991**, *10*, 1800.
(16) Schnyder, A.; Hintermann, L.; Togni, A. *Angew. Chem., Int. Ed. Engl.* **1995**, *35*, 931.
(17) Jedlicka, B.; Rülke, R. E.; Weissensteiner, W.; Fernández-Galán, R.; Jalón, F. A.; Manzano, B. R.; Rodríguez-de la Fuente, J.; Veldman, N.; Koijman, H.; Spek, A. L. *J. Organomet. Chem.* **1996**, *508*, 69.
(18) (a) Breutel, C.; Pregosin, P. S.; Salzmann, R.; Togni, A. *J. Am. Chem. Soc.* **1994**, *116*, 4067. (b) Pregosin, P. S.; Salzmann, R.; Togni, A. *Organometallics* **1995**, *14*, 842. (c) Togni, A.; Burckhardt, U.; Gramlich, V.; Pregosin, P. S.; Salzmann, R. *J. Am. Chem. Soc.* **1996**, *118*, 1031. (d) Pregosin, P. S.; Salzmann, R. *Coord. Chem. Rev.* **1996**, *155*, 35.

Table 1. ^{1}H NMR Selected Data for the Aminophosphine Ligands in Complexes Pd(N-P)(alkene) (1−4) and [Pd(2-Me-allyl)(N-P)]Tf (5 and 6)[a]

complex	amt,[b] %	C_5H_5	C_5H_n[c]	NMe_2	$H_{1'}$	$C_{1'}Me$	*ortho* Ph up[d]	*ortho* Ph down[d]
1M	66	3.70 (s)	3.85 (m) 4.01 (d), $^3J_{HH}$ = 2.2	2.96 (s) 2.55 (s)	3.02 (m)		7.22 (m)	7.67 (m)[f]
1m	34	3.69 (s)	3.80 (m) 4.02 (d), $^3J_{HH}$ = 2.2	2.84 (s) 2.61 (s)	3.02 (m)		7.12 (m)	7.58 (m)[f]
2M	78	3.95 (s)	3.89 (m) 4.06 (d), $^3J_{HH}$ = 2.2	2.96 (s) 2.72 (s)	3.08 (m)		7.42 (pt)	7.90 (m)
2m	22	3.73 (s)	3.83 (m) 4.03 (d), $^3J_{HH}$ = 2.1	3.05 (s) 2.77 (s)	3.08 (m)		7.50 (pt)	7.63 (m)
3M	73	3.28 (s)	3.73 (m) 3.90 (m) 3.93 (m)	2.92 (s) 2.16 (s)	3.15 (q)	0.81 (d), $^3J_{HH}$ = 6.3	7.17 (m)	7.68 (m)
3m	27	3.35 (s)	3.80 (m) *e*	2.88 (s) 2.14 (s)	3.15 (q)	0.67 (d), $^3J_{HH}$ = 6.3	7.09 (m)	7.78 (m)
4M	55	3.45 (s)	3.87 (m)[f] 3.92 (m)[f]	3.15 (s)[f] 3.09 (s)[f]	*e*	1.0 (d), [f] $^3J_{HH}$ = 6.1 0.9 (d), [f] $^3J_{HH}$ = 6.1	7.29 (pt)	8.04 (m)
4m	45	3.49 (s)	3.97 (m)[f] 4.05 (m)[f]	2.39 (2s)[f]			7.48 (pt)	7.78 (m)
5M	55	4.18 (s)	4.81 (3m)[f]	3.51 (s) 3.18 (s)	3.60 (m)		7.26 (m)[f]	7.85 (m)
5m	45	4.02 (s)	4.08 (m)[f]	3.46 (s) 3.34 (s)	3.79 (m)		7.26 (m)[f]	7.78 (m)
6M	54	3.76 (s)	4.65 (2m)[f] 4.68 (2m)[f]	3.50 (s) 2.77 (s)	4.30 (q)	1.52 (d), $^3J_{HH}$ = 6.6	7.23 (m)[f]	8.28 (m)
6m	46	3.75 (s)	4.73 (2m)[f]	3.54 (s) 2.99 (s)	3.88 (q)	1.49 (d), $^3J_{HH}$ = 6.6	7.28 (m)[f]	8.00 (m)

[a] Recorded at 233 K in toluene-d_8 (**1**−**4**), acetone-d_6 (**5**, **6**) or chloroform-*d* for the *ortho* phenyl protons of **1** and **3**. M = major isomer; m = minor isomer. For the adopted numbering scheme, see Chart 1. Proton resonances for 2′-, 3′-, and 4′-positions are in the range 2.75−0.6 ppm. Phenyl protons are in the range 8.2−6.8 ppm. Coupling constants are given in hertz. [b] Percentage of the isomers. [c] n = 2 for PTFA; n = 3 for PPFA. [d] Up and down refers to the phenyl groups oriented away from or toward the ferrocenyl unit, respectively. [e] Signals not identified or signals not measurable. [f] Signals for the two isomers are not clearly distinguished.

rivatives, such a mixture of diastereomers has been observed previously by us[17] for olefin complexes and by others (see, for example, ref 18c) for allyl complexes.

A different ratio of isomers (M = major isomer, m = minor isomer) has been found in each case, deduced from the ^{1}H NMR spectra (see Table 1). At low temperature (233 K) nearly all signals of the ^{1}H NMR spectra (toluene-d_8 for **1**−**4** and acetone-d_6 for **5** and **6**) of both isomers of each complex have been assigned. (See Tables 1−3 for the signal assignment at 233 K). The two equivalent amino methyl groups of the free ferrocenyl ligands are transformed into two diastereotopic groups after the N-coordination, and thus, two different singlets are always observed. The alkene protons (see Table 2) of the MA and DMFU groups give two separated signals shifted to lower frequency with respect to the free olefins.[19] These shifts are in the range usually observed for other zerovalent ML_2(alkene) complexes of palladium and platinum.[20] The signals are assigned according to the coupling constants J_{H-P}, expected to be larger for *trans* than for *cis* interactions, and by means of INDOR experiments. In all cases the protons *trans* to phosphorus appear at lower frequency. Complexes **5** and **6** show four different allyl protons for each isomer, reflecting the asymmetric environment in their coordi-

Chart 2. Observed Diastereomers of 1−6: (a) 1M-m and 3M-m; (b) 2M-m and 4M-m; (c) 5M-m and 6M-m[a]

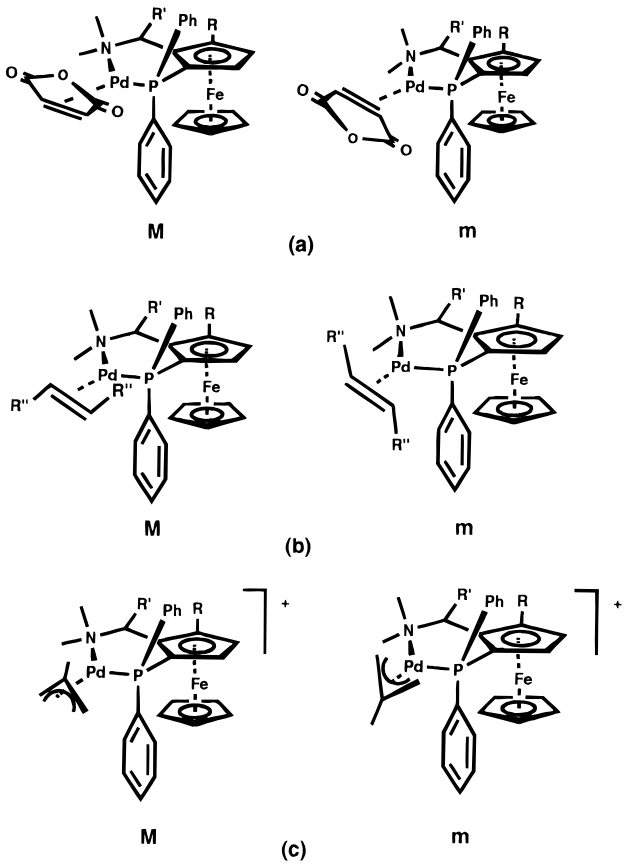

[a] R = H, R′ = Me (PPFA); R-R′ = $CH_2CH_2CH_2$ (PTFA); R″ = CO_2Me. Conformation of major (M) and minor (m) isomers has been elucidated by NOE studies (see text).

(19) ^{1}H (^{13}C) NMR data for the free alkenes in $CDCl_3$: MA, 7.04 (137.1) ppm; DMFU, 6.86 (133.9)ppm.

(20) (a) Cenini, S.; Ugo, R.; La Monica, G. *J. Chem. Soc. A* **1971**, 409. (b) Otsuka, S.; Yoshida, T.; Tatsuno, Y. *J. Am. Chem. Soc.* **1971**, *93*, 6462. (c) Ito, T.; Hasegawa, S.; Takahashi, Y.; Ishii, Y. *J. Organomet. Chem.* **1974**, *73*, 401. (d) Ittel, S. D.; *Inorg. Chem.* **1977**, *16*, 2589. (e) Itoh, K.; Ueda, F.; Hirai, K.; Ishii, Y. *Chem. Lett.* **1977**, 877. (f) Chicote, M. T.; Green, M.; Spencer, J. L.; Stone, F. G. A.; Vicente, J. *J. Chem. Soc., Dalton Trans.* **1979**, 536. (g) Cavell, K. J.; Stufkens, D. J.; Vrieze, K. *Inorg. Chim. Acta* **1980**,*47*, 67. (h) van Asselt, R.; Elsevier, C. J.; Smeets,W. J. J.; Spek, A. L. *Inorg. Chem.* **1994,** *33*, 1521.

Table 2. Selected ^{1}H and ^{13}C NMR Data for the Alkene Ligands of Complexes Pd(N-P)(alkene) (1−4)[a]

	^{1}H NMR			^{13}C NMR				
	olef H			olef C		CO		
complex	cis P	trans P	CO_2Me	cis P	trans P	cis P	trans P	CO_2Me
1M	4.24 (pt), J_{HP} = 4.0, $^3J_{HH}$ = 4.0	3.46 (dd), J_{HP} = 10.0		47.54	49.82, J_{CP} = 30.0	172.73	171.06, J_{CP} = 4.6	
1m	4.54 (pt), J_{HP} = 3.7, $^3J_{HH}$ = 3.7	3.71 (dd), J_{HP} = 10.0		47.91	48.93, J_{CP} = 30.6	172.49	171.12, J_{CP} = 4.6	
2M	5.25 (dd), J_{HP} = 1.9, $^3J_{HH}$ = 9.8	4.38 (pt), J_{HP} = 9.8	3.73 (s) 3.34 (s)	50−52.5[b]	50−52.5[b]	174.16, J_{CP} = 2.2	173.26, J_{CP} = 6.4	50−52.5[b]
2m	4.90 (dd), J_{HP} = 1.9, $^3J_{HH}$ = 10.0	4.45 (pt), J_{HP} = 10.0	3.59 (s) 3.34 (s)	50−52.5[b]	50−52.5[b]	*c*	*c*	50−52.5[b]
3M	3.77 (pt), J_{HP} = 3.8, $^3J_{HH}$ = 3.8	3.36 (dd), J_{HP} = 10.3		48.41	49.23, J_{CP} = 29.7	172.54	170.89, J_{CP} = 5.8	
3m	4.40 (pt), J_{HP} = 3.8, $^3J_{HH}$ = 3.8	3.73 (dd), J_{HP} = 10.3		47.86	48.12, J_{CP} = 30.2	169.23	*c*	
4M	5.16 (dd), J_{HP} = 2.3, $^3J_{HH}$ = 10.0	4.33 (pt), J_{HP} = 10.0	3.76 (s)[d] 3.47 (s)[d]	50.6−51.5[b]	50.6−51.5[b]	172.86	172.86	50.21
4m	4.51, $^3J_{HH}$ = 9.5	4.44, $^3J_{HP}$ = 9.5	3.38 (s)[d] 3.11 (s)[d]	50.6−51.5[b]	50.6−51.5[b]	172.86	172.86	50.05

[a] ^{1}H NMR spectra recorded at 233 K in toluene-d_8 and ^{13}C NMR at room temperature in benzene-d_6 (**2**−**4**) or chloroform-*d* (**1**). M = major isomer; m = minor isomer; pt = pseudotriplet. Coupling constants are in hertz. [b] Signals including two amino methyls and olefinic carbons. [c] Not observed. [d] Signals for the two isomers are not clearly distinguished.

Table 3. ^{1}H and ^{13}C NMR Data for the Allyl Group in [Pd(2-Me-allyl)(N-P)]Tf (5, 6)[a]

	^{1}H					^{13}C			
						CH_2			
complex	Me	H_s cis P	H_a cis P	H_s trans P	H_a trans P	cis P	trans P	Me	−*C*=
5M	1.97 (s)	2.60 (bs)[c] 3.21 (bs)[c]		4.89 (m)	4.35 (d), J_{HP} = 9.3	52.99	86.36, J_{CP} = 30.7	23.20	123.04
5m	2.36 (s)	3.28 (bs)[c]	*b*	*b*	4.16 (d), J_{HP} = 9.0	53.71	86.36, J_{CP} = 30.7	23.52	118.78
6M	1.43 (s)	2.70 (m)	3.12 (s)	4.55 (m)	4.01 (d), J_{HP} = 9.5	56.84	82.51, J_{CP} = 29.2	22.79	123.06
6m	2.28 (s)	3.45 (m)	*b*	4.82 (m)	3.96 (d), J_{HP} = 8.8	54.38	83.99, J_{CP} = 30.2	17.82	118.80

[a] ^{1}H NMR spectra recorded at 233 K in acetone-d_6 and ^{13}C NMR at room temperature in chloroform-*d*. M = major isomer; m = minor isomer. Coupling constants are in hertz. [b] Not observed. [c] Signals for the two isomers are not clearly distinguished.

nation (see Table 3). Their assignment is based on their characteristic chemical shifts[21a] and on NOE studies.

The orientation of the olefin and allyl ligands for the major and minor isomers of complexes **1**−**6** has been determined by means of NOE studies at 233 K. The MA complexes (**1** and **3**) are not soluble enough in toluene-d_8 to allow NOE measurements; hence, chloroform-d solutions have been used. In all of the complexes an NOE was found from the nonfunctionalized Cp ring to the *ortho* protons of one phosphino phenyl ring. Consequently, this Ph group must be in close proximity to the Cp ring situated below the palladium coordination plane (see Chart 2). Further NOEs were observed from these *ortho* protons to the olefin protons *cis* to phosphorus in the major isomers (M) of the MA (**1** and **3**) and DMFU (**2** and **4**) complexes, suggesting these olefin protons to be positioned below the palladium coordination plane with the endocyclic oxygen of MA pointing above the ferrocene core, while in the DMFU complexes the olefin is coordinated with its *Re* face to the (*S*,*R*)-PPFA or (*R*,*R*)-PTFA palladium units. For the π-allyl complexes (**5** and **6**), there is an NOE between the already noted *ortho* phenyl protons and the allylic methyl of the minor isomers, which indicates that the C−Me bond points toward the ferrocene unit.

Further evidence for these assignments comes from NOEs from the allyl methyl groups of the major isomers of **5** and **6** and also from the olefin proton *cis* to phosphorus of the minor isomer of **3** to the *ortho* protons of the respective upper phenyl rings.

^{13}C NMR data (see Tables 2−4) are in accordance with the structure expected for the complexes. The amino methyl groups of each isomer appear as two signals, one shifted to lower field by 10−14 ppm. Alkene carbons give resonances in the region of 47.5−52.5 ppm, which are strongly shifted to higher field with respect to the free alkenes[19] but are in the range observed for other palladium(0) complexes.[20] The allyl group shows two different resonances for the terminal carbons, with the carbon *trans* to phosphorus at higher frequency according to the stronger trans influence of this atom.

A unique signal is observed for each diastereomer in ^{31}P NMR spectra between 10 and 22 ppm (see Experimental Section).

Fluxional Behavior of the New Complexes. The fluxional behavior of complexes **1**−**6**, described below, has allowed us to calculate several free energies of activation for the isomer interconversion (see Table 5). These values are too high to be assigned to conformational changes of the chelate ring, a process that, although feasible, is expected to be of lower energy. In fact, an activation barrier of about 38 kJ mol^{-1} at 200 K has been found in the case of the PPFA−$PdCl_2$ complex.[22] In contrast to our complexes, this derivative is not expected to have different isomers depending on the orientation of the ancillary ligands and the observed barrier is attributed to a conformational change of the

(21) (a) Wilkinson, G.; Stone, F. G. A.; Abel, E. W. Eds. *Comprehensive Organometallic Chemistry*; Pergamon Press: Oxford, U.K., 1982; Vol. 6, p 409. (b) *Ibid*. Vol. 3, pp 103−109.

(22) Kalchhauser, H.; Weissensteiner, W. Unpublished results.

Table 4. Selected ^{13}C NMR Data for the Aminophosphine Ligands in Complexes Pd(N-P) (alkene) (1−4) and [Pd(2-Me-allyl)(N-P)]Tf (5, 6)[a]

compd	1′	2′, 3′, 4′	4, 5	1	2	3	N*Me*$_2$	Cp	C1′(*Me*)
1M	61.29	25.19 22.37 20.06	69.30 69.80, J_{CP} = 3.6	90.31, J_{CP} = 22.5	66.27, J_{CP} = 38	90.51, J_{CP} = 8.5	52.22 42.73	71.58	
1m	60.37	25.33 22.14 20.25	69.47 69.72, J_{CP} = 3.6	89.55, J_{CP} = 22.5	66.90, J_{CP} = 40	91.48, J_{CP} = 8.2	50.32 44.33	71.29	
2M	60.35	25.85 22.53 20.64	69.85 69.60	90.76, J_{CP} = 32.2	c	91.60, J_{CP} = 8.1	50−52.5[b] 42.61	72.27	
2m	61.46	25.85 23.03 20.32	70.00 68.9	90.95, J_{CP} = 33	*c*	90.52, J_{CP} = 8.0	50−52.5[b] 43.66	72.27	
3M	70.48		72.7 69.80, J_{CP} = 4.6	95.70, J_{CP} = 24.2	*c*	63.41, J_{CP} = 3.1	51.70 46.64	70.74	16.92
3m	70.36		73.15 70.08, J_{CP} = 4.1	95.20, J_{CP} = 26.7	*c*	63.27, J_{CP} = 3.1	52.26 45.24	70.62	15.60
4M	69.60, J_{CP} = 3.4		73.05 70.05, J_{CP} = 9.1	96.18, J_{CP} = 25.2	*c*	63.53	50.5−51.5[b] 46.70	70.98	18.23
4m	69.30, J_{CP} = 3.5		73.22 70.29, J_{CP} = 8.6	97.30, J_{CP} = 25.0	*c*	63.15, J_{CP} = 3.0	50.5−51.5[b]	70.77 45.30	16.10
5M	62.58	24.63 22.27 20.10	70.94, J_{CP} = 4.5 69.37	90.60, J_{CP} = 21.0	c	91.10, J_{CP} = 9.1	55.16 45.15	71.86	
5m	62.33	24.71 22.36 20.10	71.23, J_{CP} = 4.6 69.15	90.40, J_{CP} = 21.7	c	91.42, J_{CP} = 9.0	54.18 46.01	71.77	
6M	72.72		70.60 70.49	95.67, J_{CP} = 22.2	69.25, J_{CP} = 41.4	62.89	53.51 48.00	70.93	15.46
6m	72.15		70.61 70.42	94.75, J_{CP} = 23.2	66.93, J_{CP} = 43.7	63.80	54.36 49.35	71.04	17.82

[a] Recorded at room temperature in benzene-d_6 (**2**−**4**) or chloroform-*d* (**1**, **5**, **6**). M = major isomer; m = minor isomer. For the adopted numbering scheme, see Chart 1. Coupling constants (hertz) are listed with the corresponding resonance. Phenyl carbons are in the region 139−127.1 ppm. [b] Signals including two amino methyls and olefinic carbons. [c] Signals not observed.

Table 5. Variable-Temperature ^1H NMR Data and Calculated Free Activation Energies for the Different Coalescences Observed for Complexes 1−6

complex	$\Delta\nu$ (Hz)	T (K)	$\Delta G^{\ddagger}_c$ (kJ/mol)[a]	interchanging groups
1	18.3	346	74.8 (76.7)	amino methyls (M +m)
	10.2	338	74.6 (76.5)	amino methyls (M +m)
2	52.7	330	68.2 (71.7)	alkene methyls (m)
	168.2	353	69.7 (73.4)	alkene protons (m)
	114.0	358	71.9 (75.7)	alkene methyls (M)
	250.0	373	72.6 (76.6)	alkene protons (M)
3	11.0	293	64.1 (66.5)	amino methyls (M + m)
	16.4	303	65.4 (67.9)	amino methyls (M + m)
	32.0	313	65.9 (68.5)	alkene protons (M + m)
	235.3	368	71.9 (74.9)	amino methyls (2nd coalescence)
4	250.0	298	57.6 (58.0)	alkene protons
	213.6	328	64.0 (64.6)	amino methyls
	227.3	328	63.9 (64.4)	amino methyls
5	21.5	351	75.4 (76.0)	$H_{syn,trans}$(M) ↔ $H_{syn,trans}$(m)
	37.4	359	75.6 (76.2)	nonfunctionalized Cp
	42.4	361	75.6 (76.2)	amino methyls (M +m)
6	6.6	345	77.4 (77.9)	nonfunctionalized Cp

[a] Calculated according to the Shanan-Atidi and Bar-Eli method.[30] Minor (M) to major (m) (major to minor) isomer transformations are given.

chelate ring. In the case of the PTFA−$PdCl_2$ derivative and our complexes, only a broadening of the different signals is observed at very low temperature (about 183 K) without reaching any decoalescence.

Palladium(0) Complexes. In order to study the diastereomer interconversion of the new palladium(0) (aminoferrocenyl)phosphine complexes (**1**−**4**), we have carried out variable-temperature ^1H NMR studies in toluene-d_8 solution. In the case of the MA derivatives, these diastereomers (rotamers) can interconvert, e.g., via a rotation of the alkene unit about the palladium−olefin bond. However, for an interconversion of the DMFU isomers a ligand dissociation is required (see Chart 2).

For complex **1** at 233 K all the different resonances of the two rotamers are seen. (The aliphatic ring resonances have not been elucidated completely.) Raising the temperature allows us to detect isomer interconversion because coalescence of the amino methyl and of the functionalized cyclopentadienyl protons is observed (see Table 5 for coalescence temperatures (T_c) and free energies of activation at the coalescence temperatures $\Delta G^{\ddagger}_c$ and Figure 1 for a selection of ^1H NMR spectra at different temperatures showing the amino methyl region of complex **1** and of complexes **2**−**4**, described below). The isomer interconversion may, in principle, be caused by either an olefin rotation or an olefin decoordination−coordination process, although for the former case a smaller activation barrier is expected. The $\Delta G^{\ddagger}$c values obtained are in accordance with values reported in the literature for alkene rotations of different types of complexes,[21b] especially for those of the closely related Pd(N-N)(alkene) (N-N = diimine ligands).[20h] For theoretical studies about alkene rotation see, for example, ref 23. Although, in principle, alkene dissociation could account for the isomer interconversion of **1**, such a mechanism can be excluded since

(23) (a) Albright, T. A.; Hoffmann, R.; Thibeault, J. C.; Thorn, D. L. *J. Am. Chem. Soc.* **1979**, *101*, 3801. (b) Wheebock, K. S.; Nelson, J. H.; Cusachs, L. C.; Jonassen, H. B. *J. Am. Chem. Soc.* **1970**, *92*, 5110.
(24) Jalón, F. A.; Manzano, B. R.; Otero, A.; Rodríguez-Pérez, M. C. *J. Organomet. Chem.* **1995**, *494*, 179.

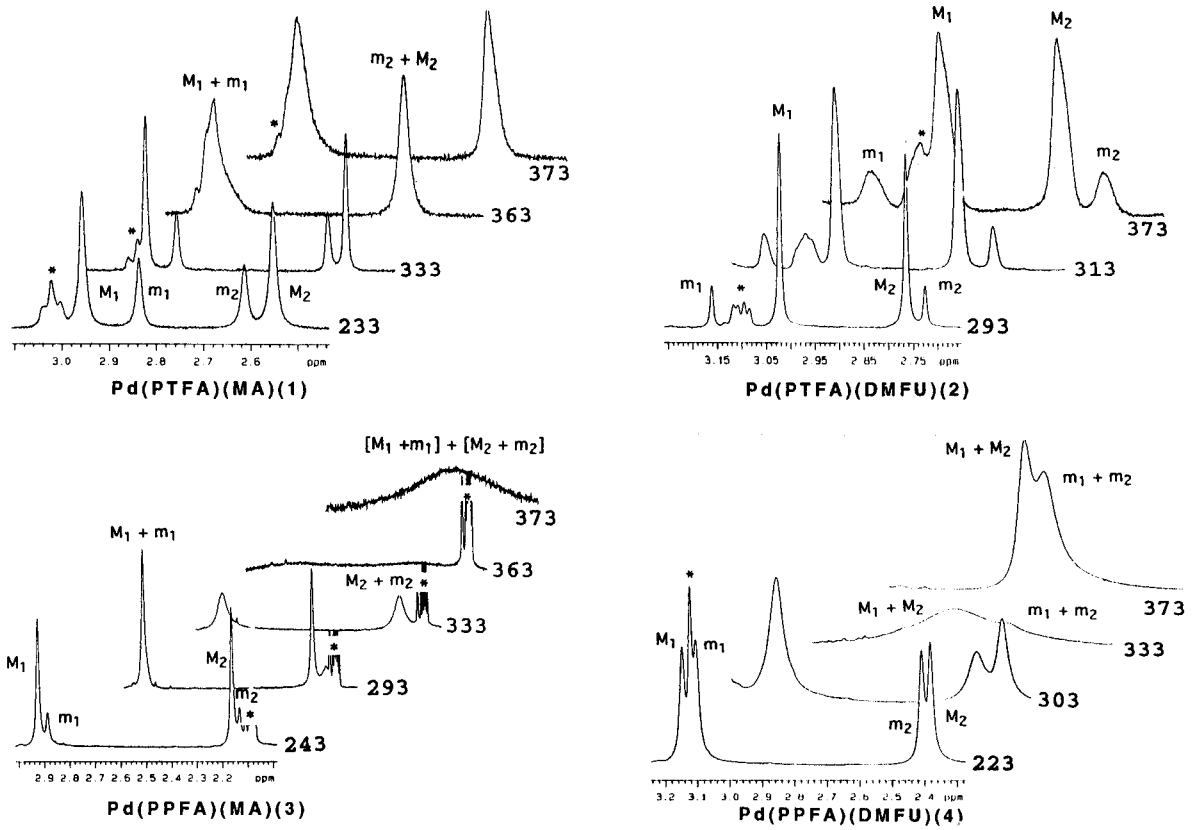

Figure 1. Variable temperature ^{1}H NMR study of complexes **1**−**4** in the amino methyl region; temperature in K; M = major isomer, m = minor isomer; subscripts 1 and 2 refer to the two diastereotopic amino methyl groups for each isomer; asterisks denote other (no amino methyl) proton resonances in the region. The following facts are noteworthy: (i) the conversion of the major (M) ↔ minor (m) diastereomers in complexes with MA (**1** and **3**) interchanges the resonances M_1 ↔ m_1 and M_2 ↔ m_2; (ii) the Pd−N bond rupture makes possible the interchanges M_1 ↔ M_2 and m_1 ↔ m_2 in complexes with the ligand PPFA (**3** and **4**); (iii) the diastereomer conversion and the Pd−N bond rupture for complex **3** transform the four low-temperature amino methyl resonances into only one signal at high temperature.

higher $\Delta G^{\ddagger}_c$ values (see discussion of complex **4** below) as well as an exchange of all olefin protons at the same time are expected. Another feasible mechanism involving dissociation and recoordination of PTFA would cause an interchange of the amino methyl groups of a like isomer, a process which was not observed up to 378 K. Hence, this interconversion mechanism must be disregarded and, consequently, we conclude that olefin rotation is the observed isomerization process.

Considering the ^{1}H NMR spectra at 233 and 243 K allows the observation of all the resonances of both isomers of complex **2.** No coalescence phenomenon corresponding to isomer interconversions could be detected up to the maximum temperature recorded. However, the alkene protons and the ester methyl groups of each isomer coalesce (see Table 5 for the $\Delta G^{\ddagger}_c$ values calculated). The different free energies of activation calculated for this complex (and also for the complexes described below) are linearly related to the coalescence temperatures. The lack of interconversion between the two isomers excludes a ligand (olefin or amino phosphine) decoordination−coordination pathway. In addition, the amino methyl groups of each isomer do not coalesce even at 373 K, the maximum temperature achieved, even though $\Delta\nu$ is small (see Figure 1). Thus, the alkene rotation is the only reasonable process to account for all the observations.

The variable temperature ^{1}H NMR study for complex **3** shows an interchange between the resonances of the minor and the major isomer. Coalescence temperatures have been measured for the amino methyl signals, and thus $\Delta G^{\ddagger}_c$ values have been calculated (see Table 5 and Figure 1). It has also been possible to detect the coalescence for a pair of alkene resonances. Because of overlap with other signals, the coalescence of the second pair of alkene signals could not be analyzed. In any case, at high temperatures a narrowing signal in a region intermediate between the two initially separated resonances is observed. Both the alkene rotation and a decoordination−coordination process of either PTFA or the olefin are feasible processes. However, the appearance of the alkene resonances at high temperature allows us to distinguish between these possibilities. In the spectrum at 373 K (far above the coalescence temperature) two different alkene signals are seen. Decoupling of ^{31}P leads to an AB system (δ_A 3.81 ppm; δ_B 3.79 ppm; J_{AB} = 4.1 Hz). A ligand decoordination−coordination process, apart from the interchange of the two isomers, would also lead to an A_2 system for these protons. Consequently, the alkene rotation seems to be the only way for the isomer interconversion. Besides the interchange of the two rotamers a new phenomenon is observed in the amino methyl region of the spectra. In contrast to the observed behavior of the complexes described previously, the four amino methyl groups are transformed, after several coalescences, to a unique large signal when the maximum temperature is achieved (see Figure 1). That means that an interconversion between the two amino methyl groups of a like isomer takes place. This interchange cannot be explained by

the alkene rotation. The only way to interconvert these signals is by amino group inversion after the rupture of the Pd−N bond. However, PPFA must remain coordinated to the palladium center via the phosphorus atom. Otherwise, a unique alkene proton signal would be observed. Surprisingly, the $\Delta G^{\ddagger}_{c}$ value calculated for this coalescence (see Table 5) fits properly with the linear plot obtained for the other coalescences noted for this system. Therefore, the activation barrier for this bond rupture process is comparable to that of the rotamer interconversion phenomenon.

For complex **4**, an isomer interconversion is not observed within the temperature range studied. For example, the unsubstituted cyclopentadienyl signals show only a small shift difference ($\delta\nu$ 24 Hz) but do not coalesce, at least up to the maximum temperature recorded (378 K). At this temperature they are slightly broadened. Thus, on the NMR time scale, neither an intermolecular alkene interchange nor an N−P ligand dissociation is observed. However, an interchange of the alkene signals (alkene protons and ester methyls) of each individual isomer is observed. At the highest temperature recorded, only one alkene proton as well as one ester methyl signal is seen for each isomer. In principle, this exchange of alkene resonances can be explained by an olefin rotation process. Besides, as for **3**, the two diastereotopic amino methyls of each individual isomer exchange. Above the coalescence temperatures corresponding to this interchange, two broad singlets are seen that narrows when the temperature is raised (see Figure 1). These observations are consistent with a Pd−N bond rupture. This process must be of lower energy than that of an olefin decoordination, a reasonable process for an isomer interconversion. In order to confirm this statement, we have monitored the transformation of pure **4M** into **4m** in toluene-d_8 at 243 K until an equilibrium ratio was reached. A $\Delta G^{\ddagger}_{243}$ value of 78 ± 2 kJ mol^{-1} is obtained, significantly higher than the values listed in Table 5. Consequently, an isomer interconversion via a decoordination−coordination mechanism takes place but is of higher energy than those processes observed by our NMR experiments.

Allyl Complexes. The variable temperature ^{1}H NMR studies for the allyl compounds **5** and **6** have been recorded at first in acetone-d_6 because these complexes are quite insoluble in toluene (see Tables 1 and 3 for the assignment of the signals at 233 K). When the temperature was increased, all the signals of **5** and **6** broadened but coalescence could not be achieved. The relatively low boiling point of the solvent prevents a complete study. Hence, further variable-temperature studies were carried out in 1,1,2,2-tetrachloroethane-d_2. For both complexes, the isomer ratio at room temperature is similar to that observed in acetone-d_6 (see Table 1); when the temperature is increased, an isomer interconversion is observed unambiguously (see below).

For **5**, an interconversion between the two isomers was observed and coalescence temperatures have been measured for the nonfunctionalized cyclopentadienyl, the $H_{syn,trans\ P}$, and also the amino methyl resonances. The two resulting signals obtained in the amino methyl region after the coalescence narrow to 413 K. This means that for like isomers an exchange of the diastereotopic amino methyls does not occur in the temperature range studied and, hence, the Pd−N bond rupture is not observed for complex **5**. (The corresponding $\Delta G^{\ddagger}_{c}$ values are listed in Table 5.) Considering possible mechanisms to account for the observed isomer interconversion, an allyl rotation in its own plane may be proposed. Although this mechanism is often put forward to account for some isomerizations in complexes of metals such as Mo, W, and Fe, it is not widely accepted for square-planar palladium complexes. Orbital considerations suggest a high activation barrier for complexes with square-planar geometries.[25] Two consecutive Berry pseudorotations in a pentacoordinate activation state could also explain allylic interconversions.[25,26] We might also consider an "apparent π-allyl rotation" mechanism similar to that proposed by other authors[15] and also by us[24] for certain allylpalladium complexes with N-donor ligands. That implies, however, a partial dissociation of the bidentate ligand. Since from the experimental data a Pd−N bond rupture can be rejected, such a mechanism would involve a Pd−P bond rupture, a process which is very unlikely, considering the strong Pd−P bond. In any case, both mechanisms can be rejected for an additional reason: they would not show the observed exchange of the $H_{syn,trans\ P}$(isomer **5M**) ↔ $H_{syn,trans\ P}$(isomer **5m**) signals but would lead to an $H_{syn,trans\ P}$(isomer **5M**) ↔ $H_{syn,cis\ P}$(isomer **5m**) interchange. A $\eta^3-\eta^1-\eta^3$ rearrangement of the allyl group could explain the observed interchange, but with such a mechanism operating, the typical $H_{syn}-H_{anti}$ interconversion should also be present. Because not all allyl hydrogen interchanges were identified unequivocally from the monodimensional study, we have performed an EXSY experiment.[27] The allyl methyl groups of the two isomers show exchange cross-peaks, evidencing the isomer interconversion. Examination of the region corresponding to the allyl protons *cis* to phosphorus reveals the following exchange cross-peaks: H_{syn}(**5M**) ↔ H_{anti}(**5m**) and H_{anti}(**5M**) ↔ H_{syn}(**5m**) (see Figure 2). The region of the allyl protons *trans* to phosphorus is not resolved sufficiently due to very similar chemical shifts of some allyl protons and in addition due to overlap with some cyclopentadienyl resonances. In any case, the H_{syn}(**5M**) ↔ H_{syn}(**5m**) interconversion has already been observed in the monodimensional study. All these exchanges, depicted in Scheme 1, are consistent with the formation of a selective σ-allyl intermediate *cis* to phosphorus as shown in Scheme 2(i). In this intermediate, the Pd−C and C−C bond rotation (ii) and re-formation of the π form (iii) allows the H_1-H_2 interchange and the isomer interconversion. A σ-allyl intermediate *trans* to phosphorus can be excluded for complex **5,** because the interchange H_{syn}(**5M**) ↔ H_{syn}(**5m**) and H_{anti}(**5M**) ↔ H_{anti}(**5m**) is not observed in the spectral region corresponding to the allyl protons *cis* to phosphorus. Such a selective $\eta^3-\eta^1-\eta^3$ isomerization has also been reported by Pregosin et al. for chiral allyl complexes with

(25) Vrieze, K. In *Dynamic Nuclear Magnetic Resonance Spectroscopy;* Jackman, L. M., Cotton, F. A., Eds.; Academic Press: New York, 1975.

(26) (a) Crociani, B; Di Bianca, F.; Giovenco, A.; Boschi, T. *Inorg. Chim. Acta* **1987**, *127*, 169. (b) Hansson, S.; Norrby, P. O.; Sjögren, M. P. T.; Åkermark, B.; Cucciolito, M. E.; Giordano, F.; Vitagliano, A. *Organometallics* **1993**, *12*, 4940.

(27) Bodenhausen, G.; Ernst, R. R. *J. Am. Chem. Soc.* **1982**, *104*, 1304.

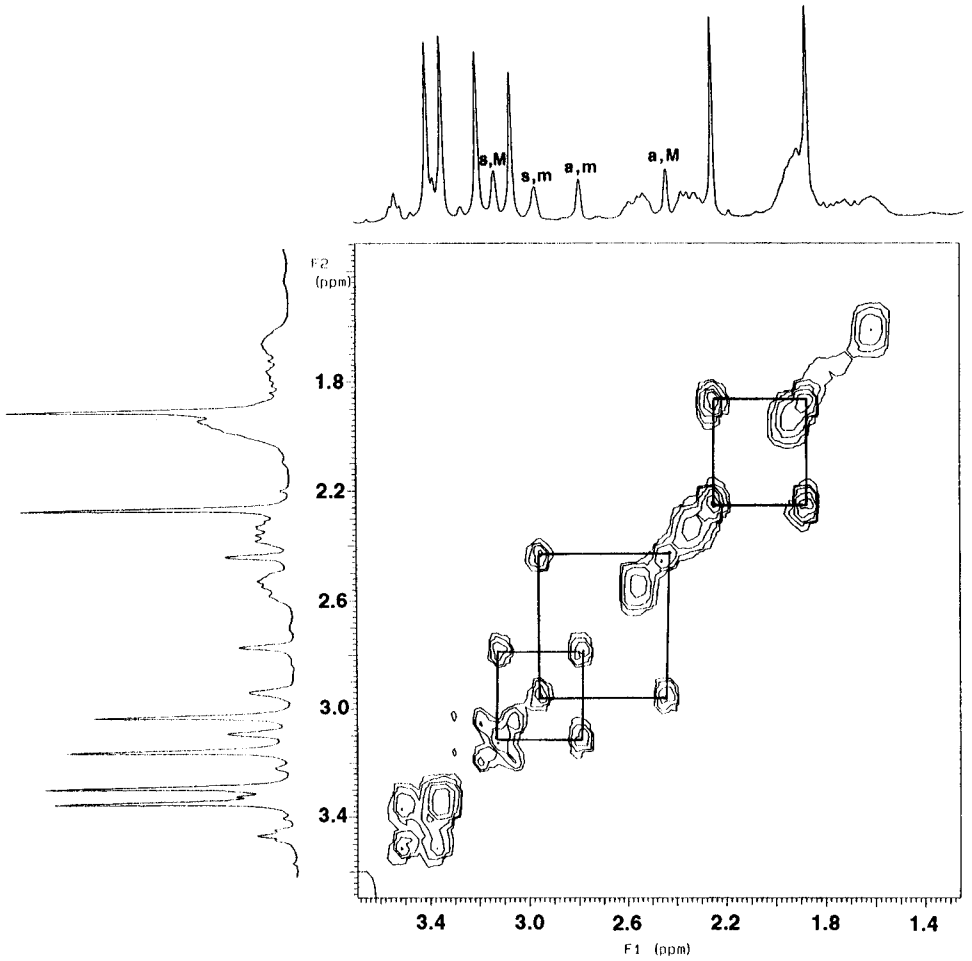

Figure 2. EXSY (1,1,2,2-tetrachloroethane-d_2, 293 K) of **5M** and **5m**, showing the exchange peaks of the allyl protons *cis* to phosphorus (s = syn; a = anti) and the allylic methyls.

Scheme 1. Observed Interchanges for 5M and 5m

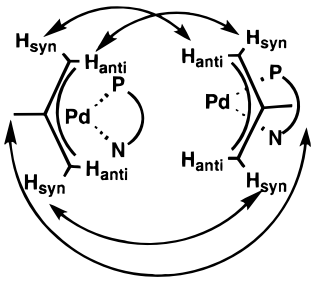

Scheme 2. Selective Syn−Anti Interchange of the Allyl Group of 5

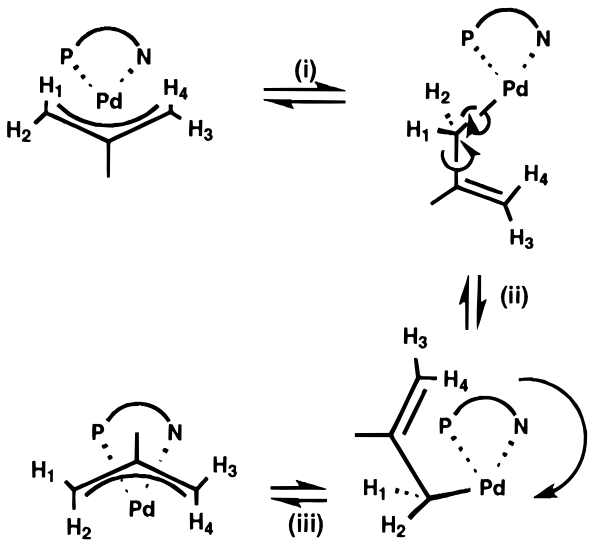

bidentate ferrocenyl diphosphine[18a,b,d] and P−S[28] ligands. Recently, Hosokawa el al.[29] also described an allylpalladium complex with a chiral P−O ligand exhibiting such a selective $\eta^3-\eta^1$ opening. Steric or electronic reasons have been suggested for such selective isomerizations. For our derivative, on the basis of steric effects, one might expect the σ-bond being formed *trans* to phosphorus. Hence, we propose that for complex **5**, where two significantly different donor atoms are present, the higher *trans* influence is responsible for the selective Pd−C bond opening *trans* to phosphorus.

In the variable-temperature ^{1}H NMR study of **6** recorded in 1,1,2,2-tetrachloroethane-d_2 only the coalescence temperature between the resonances of the nonfunctionalized cyclopentadienyl groups is clearly measured. When the temperature is raised, the initial four resonances for the amino methyl groups are transformed into only one signal, meaning that, besides the isomer interconversion, a Pd−N bond rupture takes place. Further, coalescence temperatures could not be estimated, since several signals seem to coalesce simultaneously, leading to broadening of nearly all signals

(28) Herrmann, J.; Pregosin, P. S.; Salzmann, R.; Albinati, A. *Organometallics* **1995**, *14*, 3311.
(29) Hosokawa, T.; Wakabayashi, Y.; Hosokawa, K.; Tsuji, T.; Murahashi, S.-I. *J. Chem. Soc., Chem. Commun.* **1996**, 859.

Table 6. Crystallographic Data for 4 and 6

	4	6
	Crystal Data	
chem formula	$C_{32}H_{36}FeNO_4PPd$	$C_{31}H_{35}F_3FeNO_3PPdS$
fw	691.84	751.88
cryst syst	orthorhombic	orthorhombic
color	orange	orange
space group	$P2_12_12_1$	$P2_12_12_1$
size (mm)	0.45 × 0.2 × 0.2	0.6 × 0.25 × 0.25
a (Å)	11.108(2)	9.544(2)
b (Å)	14.566(3)	15.588(3)
c (Å)	19.024(4)	21.641(4)
V (Å^3)	3078.1(11)	3219.6(11)
Z	4	4
T (K)	298	298
λ (Å)	0.710 69	0.710 69
D_{calcd} (g cm^{-3})	1.493	1.551
μ (mm^{-1})	1.144	1.173
	Data Collection	
scan limits (deg)	5−45	5−50
data colled	+11, +15, +20	+10, +18, +25
no. of indpndnt rflns	2294	2997
no. of obsd rflns	2007	1908
	Refinement[a]	
wR2	0.1272 (2994 rflns)	0.1577 (2987 rflns)
R1($F_o > 4\sigma$)	0.0484 (2007 rflns)	0.0523 (1997 rflns)
GoF	1.048	1.218
Δ/ρ (e Å^{-3})	0.95	0.57
Flack x	0.182(781)	0.1226(832)

[a] wR2 = $[\sum[w(F_o^2 - F_c^2)^2]/\sum[w(F_o^2)^2]]^{1/2}$; R1 = $\sum||F_o| - |F_c||/\sum|F_o|$; GOF = $[\sum[w(F_o^2 - F_c^2)^2]/[n - p]]^{1/2}$.

Table 7. Selected Bond Lengths (Å) and Angles (deg) for 4

	Bond Distances		
Pd1−C29	2.145(12)	N1−C26	1.619(26)
Pd1−C30	2.083(11)	C23−C24	1.485(24)
Pd1−P1	2.283(3)	C23−C10	1.552(20)
Pd1−N1	2.252(9)	C28−C29	1.437(17)
P1−C6	1.798(12)	C28−O1	1.213(14)
P1−C11	1.833(11)	C28−O2	1.374(14)
P1−C17	1.852(13)	C30−C29	1.409(16)
N1−C25	1.385(17)	C30−C31	1.476(16)
N1−C23	1.465(22)		
	Bond Angles		
C29−Pd1−C30	38.91(0.42)	N1−C23−C24	111.45(1.64)
C29−Pd1−N1	111.79(0.42)	N1−C23−C10	113.76(1.48)
C30−Pd1−P1	116.07(0.30)	C24−C23−C10	112.37(1.58)
Pd1−P1−C6	110.77(0.38)	C23−C10−C6	124.06(1.22)
C17−P1−C11	100.73(0.54)	C10−C6−P1	123.84(0.88)
C25−N1−C26	106.04(1.45)	O2−C28−C29	111.51(1.11)
Pd1−N1−C23	103.14(0.97)	C28−C29−C30	111.51(1.11)
C25−N1−C23	123.97(1.38)	C29−C30−C31	121.54(1.10)
C26−N1−C23	103.45(1.32)		

at the same time. Above 408 K the complex decomposes through an irreversible process.

X-ray Structures of Complexes Pd(PTFA)(DMFU) (4) and [Pd(PTFA)(η^3-2-Me-C_3H_4)]Tf (6). All diffraction data were collected at 298 K; structures were solved with direct methods and refined with least squares as described in the Experimental Section. Crystallographic data for **4** and **6** are summarized in Table 6; selected bond lengths and angles are given in Tables 7 and 8.

4: Complex **4** crystallizes in the orthorhombic space group $P2_12_12_1$ with four molecules in the unit cell. The molecular structure of **4** is shown in Figure 3. A discussion of the general structural features is given below. It is of interest to note that although in solution an equilibrium of two diastereomers is observed at ambient temperatures, the crystal used consisted only of one diastereomeric form.

Table 8. Selected Bond Lengths (Å) and Angles (deg) for 6

	Bond Distances		
Pd1−N1	2.117(13)	P1−C1	1.829(14)
Pd1−C27	2.121(15)	N1−C26	1.489(20)
Pd1−C28	2.180(15)	N1−C25	1.516(19)
Pd1−C29	2.216(13)	N1−C23	1.519(20)
Pd1−P1	2.287(4)	C23−C8	1.495(19)
P1−C9	1.809(13)	C23−C24	1.548(24)
P1−C17	1.829(15)		
	Bond Angles		
C27−Pd1−C29	66.46(0.64)	N1−C23−C24	112.39(1.5)
C27−Pd1−P1	96.87(0.46)	N1−C23−C8	117.96(1.27)
C29−Pd1−N1	98.31(0.61)	C24−C23−C8	107.73(1.43)
Pd1−P1−C9	111.62(0.44)	C23−C8−C9	127.20(1.23)
C11−P1−C17	105.19(0.64)	C8−C9−P1	124.20(0.93)
C25−N1−C26	106.09(1.30)	C27−C28−C30	122.61(1.66)
Pd1−N1−C23	117.15(0.98)	C27−C28−C29	116.20(1.67)
C25−N1−C23	106.38(1.33)	C29−C28−C30	119.91(1.87)
C26−N1−C23	108.02(1.26)		

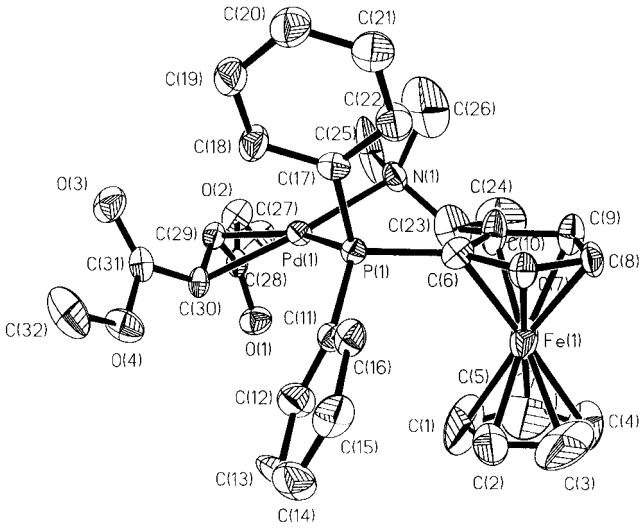

Figure 3. Molecular structure of **4** in the crystal.

6: Crystals of the cationic complex belong to the orthorhombic space group $P2_12_12_1$ with four molecules in the unit cell. The molecular structure of the cation (the noncoordinating anion has been omitted for clarity) is shown in Figure 4. Even from a visual comparison it is obvious that the conformations of **4** and **6** differ significantly from each other. The general structural features of the ferrocene units of **4** and **6** are very similar: the average Fe−C_{ar} bond lengths are 2.01(3) Å for **4** and 2.03(3) Å for **6**, and the average C_{ar}−C_{ar} bond lengths are 1.36(8) and 1.40(5) Å, respectively. The ferrocenyl cyclopentadienyl (Cp) rings are slightly tilted with respect to each other by 3.2 (**4**) and 5.8° (**6**). Significant differences, however, are seen in the side-chain conformations and in the orientation of the square-planar-substituted palladium unit. In both **4** and **6**, the palladium is located below the plane of the substituted Cp ring (0.17, and 0.05 Å, respectively). However, the six-membered palladium chelate rings of **4** and **6** adopt different molecular conformations as well. In **4** the chelate ring shows a twisted conformation with the dimethylamino nitrogen 0.56 Å above Cp[1] and with the side-chain methyl group C(24) in a pseudoequatorial position (C(24) 0.48 Å below Cp[1]), while in **6** C(24) is in a pseudoaxial (1.90 Å above Cp[1]) conformation, but in this case the amino nitrogen is located 0.29 Å below Cp[1]. Bond lengths and bond angles of the square-planar

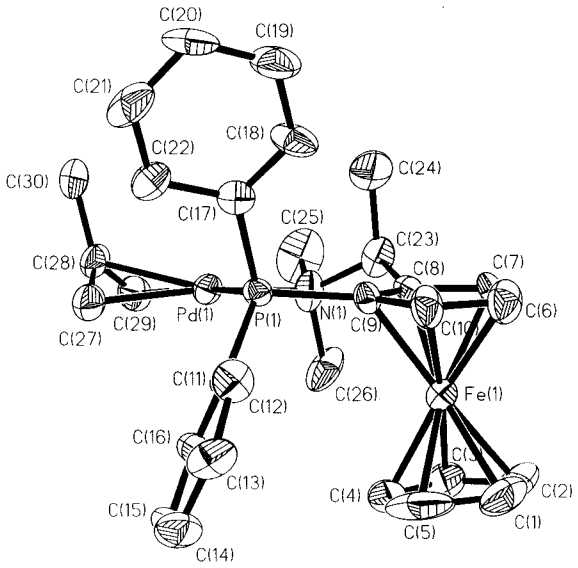

Figure 4. Molecular structure of **6** in the crystal.

palladium units of **4** and **6** show similar trends: the N−Pd−P bond angles are slightly opened up (95° in **4** and 97° in **6**), and the bonds from palladium to those carbons *trans* to the coordinated phosphorus are longer than those *trans* to the nitrogen (0.06 Å in **4** and 0.09 Å in **6**), indicating a stronger trans influence of phosphorus as compared to nitrogen.

In conclusion, the X-ray structures of **4** and **6** show that in palladium complexes the PPFA ligand can adopt different conformations depending on the additional ligands coordinated to the palladium atom.

As mentioned above, in contrast to the case for the solid state, in solution two isomers are observed in equilibrium for each complex, **4** and **6**. These isomers differ in the way either the alkene (**4**) or the allyl group (**6**) is attached to the remaining PPFA−palladium unit. According to the NMR assignments the molecular structures found in the solid state are those which also predominate in solution.

In summary, from the results discussed above, it is obvious that the fluxional behavior of both alkene−palladium(0) and allyl−palladium(II) derivatives strongly depends on the coordinated aminophosphine ligand. For all PPFA complexes a Pd−N bond rupture was observed, while for PTFA complexes such a process must be of higher energy. This could be caused by the stronger chelating effect expected for the PTFA ligand. We have shown for the first time that for (aminoferrocenyl)-phosphine palladium complexes Pd−N bond cleavage processes can take place not only for Pd(0) but also for Pd(II) species. This is in agreement with the original proposal by Hayashi for PPFA type complexes. Whether PTFA type analogues behave similarly in the actual catalysis reaction is currently under investigation.

Experimental Section

General Comments. All manipulations were carried out under an atmosphere of dry oxygen-free nitrogen using standard Schlenk techniques. Solvents were distilled from the appropriate drying agents and degassed before use. Elemental analyses were performed with a Perkin-Elmer 2400 microanalyser. IR spectra were recorded as KBr pellets with a Perkin-Elmer PE 883 IR spectrometer. ^{1}H, ^{13}C, and ^{31}P-NMR spectra were recorded on a Varian Unity 300 spectrometer. Chemical shifts (ppm) are given relative to TMS (^{1}H, ^{13}C NMR) and 85% H_3PO_4 (^{31}P NMR). The NOE difference spectra were recorded with the following acquisition parameters: spectral width 5000 Hz, acquisition time 3.27 s, pulse width 90°, relaxation delay 4 s, irradiation power 5−10 dB. The EXSY spectrum was obtained using a standard three-pulse sequence. The mixing time was 0.8 s. For variable-temperature spectra, the probe temperature (±1 K) was controlled by a standard unit calibrated with a methanol reference. Free energies of activation were calculated from the coalescence temperature (T_c) and the frequency difference between the coalescing signals in the limit of slow exchange with the formula[30] $\Delta G^{\ddagger}_c = aT(10.319 + \log T/k)$. k values were calculated according to the Shanan-Atidi and Bar-Eli method.[30] The estimated error in the calculated free energies of activation is 1.0−1.1 kJ mol^{-1}.

$Pd_2(dba)_3{\cdot}CHCl_3$ and $[Pd(\eta^3\text{-}2Me\text{-}C_3H_4)Cl]_2$ were prepared according to literature methods.[31,32] Complex **1** has been previously described by us.[17]

Preparation of Pd(PTFA)(DMFU) (2). To a degassed solution of $Pd_2(dba)_3{\cdot}CHCl_3$ (100.0 mg, 0.09 mmol) in 20 mL of toluene are added 99.3 mg (0.21 mmol) of PTFA and 30.5 mg (0.21 mmol) of dimethyl fumarate. The solution is stirred for 14 h, filtered, and evaporated to dryness. The residue is washed with hexane (3 × 25 mL) and dried in vacuo, yielding an orange solid. Yield: 51.0 mg (0.071 mmol, 39%). Anal. Calcd for $C_{34}H_{38}FeNO_4PPd$: C, 56.89; H, 5.33; N, 1.95. Found: C, 56.74; H, 5.44; N, 1.92. IR: ν(C=C) 1570 cm^{-1}; ν(C=O) 1685 cm^{-1}, 1670 cm^{-1}. ^{31}P NMR (benzene-d_6): 12.09 (s).

Preparation of Pd(PPFA)(MA) (3). The procedure is identical with that described for **2.** Amounts are as follows: $Pd_2(dba)_3{\cdot}CHCl_3$, 113 mg, (0.109 mmol); PPFA, 114.0 mg (0.262 mmol); MA, 25.6 mg (0.262 mmol). **3** is obtained as an orange solid. Yield: 62.0 mg (0.096 mmol, 46%). Anal. Calcd for $C_{30}H_{30}FeNO_3PPd$: C, 55.80; H, 4.68; N, 2.17. Found: C, 55.26; H, 4.68; N, 2.15. IR: ν(C=C) 1571 cm^{-1}; ν(C=O) 1781, 1723 cm^{-1}. ^{31}P NMR (toluene-d_8): 12.21 (s) (**3M**); 21.90 (s) (**3m**).

Preparation of Pd(PPFA)(DMFU) (4). The procedure is identical with that described for **2.** Amounts are as follows: $Pd_2(dba)_3{\cdot}CHCl_3$, 150.0 mg (0.144 mmol); PPFA, 153.5 mg (0.347 mmol); DMFU, 50.1 mg (0.347 mmol). **4** is obtained as an orange solid. Yield: 62.0 mg (0.09 mmol, 46%). Anal. Calcd for $C_{32}H_{36}FeNO_4PPd$: C, 55.57; H, 5.25; N, 2.03. Found: C, 55.22; H, 5.17; N, 2.20. IR: ν(C=C) 1567 cm^{-1}; ν(C=O) 1691, 1671 cm^{-1}. ^{31}P NMR (benzene-d_6): 10.71 (s) (**4M**), 10.00 (s) (**4m**).

Preparation of [Pd(η^3-2-Me-C_3H_4)Pd(PTFA)]Tf (5). The allylic complexes are prepared in a way similar to that described by Pregosin.[18a−c] To a degassed solution of 237.4 mg (0.254 mmol) of $[Pd(\eta^3\text{-}2\text{-}Me\text{-}C_3H_4)Cl]_2$ and 100 mg (0.254 mmol) of PTFA in 20 mL of CH_2Cl_2 is added a solution of $AgCF_3SO_3$ (99%; 131.8 mg, 0.508 mmol) in 2 mL of CH_3OH. After it is stirred for 1 h in the dark, the orange solution is filtered over a plug of Celite and evaporated to dryness. The gummy residue is triturated with hexane and diethyl ether, giving an orange solid. Yield: 353 mg (0.454 mmol, 89%). Anal. Calcd for $C_{33}H_{37}F_3FeNO_3PPdS$: C, 50.94; H, 4.79; N, 1.80. Found: C, 50.72; H, 4.74; N, 1.82. ^{31}P NMR (1,1,2,2-tetrachloroethane-d_2): 21.09 (s).

Preparation of [Pd(η^3-2-Me-C_3H_4)Pd(PPFA)]Tf (6). The procedure is identical with that described for **5**; 224.08 mg (0.508 mmol) of PPFA is used. Yield: 312 mg (0.415 mmol, 82%). Orange crystals were obtained by vapor diffusion from CH_2Cl_2/Et_2O. Anal. Calcd for $C_{31}H_{35}F_3FeNO_3PPdS$: C, 49.52;

(30) Sandström, J. *Dynamic NMR Spectroscopy*; Academic Press: London, 1982.
(31) Ukai, T.; Kawazura, H.; Ishii, Y., Bonnet, J. J.; Ibers, J. A. *J. Organomet. Chem.* **1974**, *65*, 253.
(32) Dent, W. T.; Wilkinson, A. J. *J. Chem. Soc.* **1964**, 1585.

H, 4.69; N, 1.86. Found: C, 49.37; H, 4.76; N, 1.84. ^{31}P NMR (acetone-d_6): 18.06 (s) (**6M**), 20.02 (s) (**6m**).

X-ray Structural Analyses. Complex 6. A crystal of approximate dimensions of 0.6 × 0.25 × 0.20 mm was mounted in a glass capillary. Intensity data were collected on a modified Stoe diffractometer (Mo Kα radiation, graphite monochromator, $\lambda = 0.710\ 69$ Å) at ambient temperature (298 K). Cell parameters were obtained by least-squares refinement against the setting angles of 62 reflections with $15° \leq 2\theta \leq 32°$. Crystals were orthorhombic, space group $P2_12_12_1$, with four formula units in the unit cell. Cell dimensions: $a = 9.544(2)$ Å, $b = 15.588(3)$ Å, $c = 21.641(4)$ Å, $V = 3219.6(11)$ Å^3, $d_{calcd} = 1.551$ g/cm^3. A total of 2997 unique reflections were collected ($0 \leq h \leq 10$, $0 \leq k \leq 18$, $0 \leq l \leq 25$, $2\theta_{max} = 50°$), of which 1908 were significant with $I/\sigma(I) > 4$. Data were empirically corrected for absorption.[33]

The structure was solved using direct methods.[34] One molecule of triflic acid was included into the model, and all non-hydrogen atoms were refined anisotropically. Full-matrix least-squares refinement[35] of 383 parameters against all data converged at the following values for reliability indices: $wR2 = [\sum[w(F_o^2 - F_c^2)^2]/\sum[w(F_o^2)^2]]^{1/2} = 0.1577$ for 2987 reflections; $R1 = \sum||F_o| - |F_c||/\sum|F_o| = 0.0523$ for 1908 reflections with $F_o > 4\sigma(F_o)$ and 0.1160 for all reflections. Goodness-of-fit $S = [\sum[w(F_o^2 - F_c^2)^2]/[n - p]]^{1/2} = 1.218$ ($n = 2987$, number of observations; $p = 383$, number of parameters). The maximum and minimum electron densities in the final difference electron density map were 0.57 and −0.49 e/Å^3. The absolute structure parameter[36] converged to a value of 0.1226 with an esd of 0.0832.

(33) Walker, N.; Stuart, D. *Acta Crystallogr.* **1983**, *A39*, 158.
(34) SHELXTL 5.0, Siemens Crystallographic Research System, 1994.
(35) Sheldrick, G. M. SHELXL-93, a Program for the Refinement of Crystal Structures from Diffraction Data; University of Göttingen, Göttingen, Germany, 1993.
(36) Flack, H. D. *Acta Crystallogr.* **1983**, *A39*, 876.

Complex 4. Data collection and structure solution were performed in a similar manner as for **6**. A crystal of approximate dimensions of 0.45 × 0.2 × 0.2 mm was mounted in a glass capillary, and data were collected at room temperature (298 K). Cell parameters were obtained from 72 reflections with $15 \leq 2\theta \leq 24°$. Crystals were orthorhombic, space group $P2_12_12_1$ with four formula units in the unit cell. Cell dimensions: $a = 11.108(2)$ Å, $b = 14.566(3)$ Å, $c = 19.024(4)$ Å, $V = 3078.1(11)$ Å^3, $d_{calcd} = 1.493$ g/cm^3. A total of 2294 unique reflections were collected ($0 \leq h \leq 11$, $0 \leq k \leq 15$, $0 \leq l \leq 20$, $2\theta_{max} = 45°$), of which 2007 were significant with $I/\sigma(I) > 4$. Data were corrected for absorption.[33]

All non-hydrogen atoms were refined anisotropically. Refinement converged at the following reliability values: $wR2 = 0.1272$ for 2994 reflections, $R1 = 0.0484$ for 2007 reflections with $F_o > 4\sigma(F_o)$ and 0.0602 for all reflections. Goodness-of-fit $S = 1.048$. The maximum and minimum electron densities in the final difference electron density map were 0.95 and −1.07 e/Å^3. The absolute structure parameter converged to a value of 0.1821 with an esd of 0.0781.

Acknowledgment. This study was supported by the Dirección General de Investigación Científica y Técnica (DGICYT, Grants PB92-0715 and PB95-0901 and Acciones Integradas HU93-016 and HU94-009, Cuidad Real, Spain), the Fonds zur Förderung der Wissenschaftlichen Forschung (Project P09859-CHE), and Österreichischer Akademischer Austauschdienst (ÖAD, Acciones integradas projects 39/94 and 29/95, Wien, Austria).

Supporting Information Available: Tables of positional and atomic displacement parameters for all atoms, anisotropic thermal parameters, bond lengths and angles, and least-squares planes and atomic deviations for complexes **4** and **6** (25 pages). Ordering information is given on any current masthead page.

OM9610354